

# Inorganic Nanoparticles and the Immune System: Detection, Selective Activation and Tolerance

Neus G. Bastús<sup>a,\*</sup>, Ester Sánchez-Tilló<sup>b</sup>, Silvia Pujals<sup>c</sup>, Joan Comenge<sup>a</sup>, Ernest Giralt<sup>c</sup>, Antonio Celada<sup>b</sup>, Jorge Lloberas<sup>b</sup>, and Victor F. Puntes<sup>a,d</sup>

a-Institut Català de Nanotecnologia, Campus UAB Bellaterra,,08193 Barcelona, Spain

b- Macrophage Biology Group, Institute for Research in Biomedicine, Barcelona Science Park and Department of Physiology, University of Barcelona, Barcelona, Spain.

c- Design Synthesis and Structure of Peptides and Proteins, Institute for Research in Biomedicine, Barcelona Science Park, Barcelona, Spain

d- Institut de Recerca i Estudis Avançats (ICREA)

\* e-mail: (N.G.B) neus.bastus@icn.cat

## ABSTRACT

The immune system is the responsible for body integrity and prevention of external invasion. On one side, nanoparticles are no triggers that the immune system is prepared to detect, on the other side it is known that foreign bodies, not only bacteria, viruses and parasites, but also inorganic matter, can cause various pathologies such as silicosis, asbestosis or inflammatory reactions. Therefore, nanoparticles entering the body, after interaction with proteins, will be either recognized as self-agents or detected by the immune system, encompassing immunostimulation or immunosuppression responses. The nature of these interactions seems to be dictated not specially by the composition of the material but by modifications of NP coating (composition, surface charge and structure). Herein, we explore the use of gold nanoparticles as substrates to carry multifunctional ligands to manipulate the immune system in a controlled manner, from undetection to immunostimulation. Murine bone marrow macrophages can be activated with artificial nanometric objects consisting of a gold nanoparticle functionalized with peptides. In the presence of some conjugates, macrophage proliferation was stopped and pro-inflammatory cytokines were induced. The biochemical type of response depended on the type of conjugated peptide and was correlated with the degree of ordering in the peptide coating. These findings help to illustrate the basic requirements involved in medical NP conjugate design to either activate the immune system or hide from it, in order to reach their targets before being removed by phagocytes. Additionally, it opens up the possibility to modulate the immune response in order to suppress unwanted responses resulting from autoimmunity, or allergy or to stimulate protective responses against pathogens.

## 1. INTRODUCTION

Despite the remarkable rapidness in the development of strategies for particle synthesis and functionalization as well as the further use of these conjugates in biomedical applications, relatively little is still stated about the interaction of nanoparticles (NPs) with living systems<sup>1-3</sup>. This is particularly important for the immune system, which is responsible for maintaining body integrity and preventing external invasion. NPs are deliberately injected to perform a specific medical application, such as fluorescent agents for imaging, drug delivery vehicles or therapeutic agents for hyperthermia treatments, or unintentionally incorporated as a consequence of manufacturing processes, combustion or consumer products. In this regard, the assessment of the adverse effects that can result from the exposure of the immune system to NPs is of vital importance to provide the basis for designing safer, and more efficient biomaterials.

The immune system is a collection of mechanisms within an organism to protect it against disease by identifying and detecting pathogens. Its main function is the self/non-self discrimination, therefore detecting a wide variety of agents, from viruses to parasites, and distinguishing them from the organism own healthy cells and tissues<sup>4</sup>. Vertebrates are endowed with an immune system with two major subdivisions, the innate or non-specific immune system, which is the first line of defense against invading organisms, and the adaptive or specific immune system, acting as a second line of defense and providing protection against re-exposure. The immediate response is carried out by the innate immune system which is not antigen specific and reacts equally well to a variety of organisms, typically triggering a protective inflammatory response within minutes. If the intruding object is not eliminated, the innate immune precedes and empowers the adaptive immune response, reacting only with the organism that induced the response.

Since NPs are no triggers that the immune system is prepared to detect, the innate immune system is supposed to first react with NPs. NPs entering the body can be either recognized as self-agents or detected by the immune system, encompassing immunostimulation or immunosuppression. responses. The former case represents the major area of interest in the area of drug delivery and several camouflaging strategies, based on their functionalization with poly(ethylene glycol) (PEG) or other types of polymers, have been reported<sup>5</sup>. Interestingly, although these strategies represent effective ways to avoid primary immune recognition, an associated problem is the formation of PEG-specific antibodies, which leads to altered pharmacokinetics of NPs after successive exposures<sup>6,7</sup>, something shown in the case of liposomes. On the other hand, when detected, the immunostimulation potential of NPs can significantly contribute to the development of improved vaccine formulations (using the NPs as vaccine adjuvants)<sup>8</sup>. The nature of these interactions seems to be dictated not only by the composition of the material but also by the morphology, surface chemistry and aggregation state of the colloidal NPs. Thus, previously reported studies show that modifications of NP coating (composition, surface charge and structure) modulates the immune response. In fact, the immune system is known to respond to inorganic particulate material as in the case of asbestosis and silicosis. However, in those cases the particles are of few microns or larger beyond the limits of frustrated phagocytosis<sup>9</sup>. These contributions have been widely reviewed by Sperling et al.<sup>10</sup>. Additionally, the initial recognition and categorization of NPs by the immune system is an essential determining factor for the fate and distribution of these materials inside the body and the interactions of NPs with some components of immune system may have a significant impact on their bioavailability and clearance<sup>11</sup>. The universal trend is that the smaller particles have a substantially longer lifetime in the blood than the larger particles. For instance, 300 nm polymer particles have a typical blood clearance time of a few minutes, while small particles (both polymeric and inorganic) of 10-20 nm may have a lifetime in the blood from a few hours to several days<sup>12,13</sup>. Moreover, the change of particle size from 240 to 80 nm showed an extension of the half-life of the particles in mice and a drug in it (TNF<sub>R</sub>) by 24-fold from 28.2 min to 11.33 h<sup>14</sup>.

In this context, we explore the use of Au NPs as substrates to carry multifunctional ligands to manipulate the immune system in a controlled manner. Thus, the main goals in this work are to study the conditions by which it is possible (i) to modulate the response of the immune system (vaccination, rejection, autoimmunity, allergies, and cancer) and (ii) to camouflage the conjugates from the immune system while trying to reach their target (when used as drug delivery vehicles or contrast agents). We show how murine bone marrow macrophages were able to recognize peptidic conjugates of Au NPs, while peptides or Au NPs alone were not recognized. Consequently, in the presence of conjugates, macrophage proliferation was stopped and pro-inflammatory cytokines such as TNF- $\alpha$ , IL-1 $\beta$ , and IL-6, as well as nitric oxide synthase (NOS2) were induced. Furthermore, macrophage activation by Au NPs conjugated to different peptides appeared to be rather independent of peptide length and polarity, but dependent on peptide pattern at the NP surface. Additionally, the biochemical type of response also depended on the type of conjugated peptide and could be correlated with the degree of ordering in the peptide coating. These findings help to illustrate the basic requirements involved in medical NP conjugate design to either activate the immune system or hide from it in order to reach their targets before being removed by phagocytes. Additionally, it opens up the possibility to modulate the immune response in order to suppress unwanted responses resulting from autoimmunity, or allergy or to stimulate protective responses against pathogens. Furthermore, the control of the activation of the innate immune system could open the possibility to design a new generation of artificial adjuvants and antigen delivery systems for vaccination.

## 2. MATERIALS AND METHODS

### 2.1 Chemicals

All chemicals used were of highest available purity, and were supplied by Merck, Sigma-Aldrich, Fluka. The Millipore water had a resistance of 18.2 MΩ cm. Recombinant M-CSF (1200 U/mL 10 ng/mL) was obtained from R&D Systems Inc. (Minneapolis, MN), and alternatively, we used L-cell conditioned medium as the source of M-CSF. All reagents were prepared following the manufacturer's recommendations.

### 2.2 Techniques

UV-visible spectra were acquired with a Shimadzu UV-2400 spectrophotometer. Dynamic light scattering (DLS) measures were made with a Malvern ZetaSizer Nano ZS instrument operating at a light source wavelength of 532 nm and a fixed scattering angle of 173°. Zeta potential was determined using a Malvern ZetaSizer analyzer. These measurements were carried out using a control pH of 7.0. Transmission electron microscopy images were recorded with a JEOL 1010 microscope which operates at 80 kV. Real time-PCR was carried out with 2X SYBR Green PCR Master Mix using the ABI Prism 7900 detection system (Applied Biosystems, Foster City, CA).

### 2.3 Synthetic Procedures

Gold nanoparticles of 10 nm to 200 nm in diameter were synthesized following previously developed strategies<sup>15-17</sup>. In detail, a solution of sodium citrate 2.2 mM in Milli-Q water (150 mL) was heated to reflux with a heating mantle in a 250 mL three-necked round-bottom flask for 15 min under vigorous stirring. After boiling had commenced, 1 mL of HAuCl<sub>4</sub> 25 mM was injected. The resulting particles were stabilized with negatively charged citrate ions and were thus well suspended. Immediately after the synthesis of the Au seeds and in the same reaction vessel, the reaction was cooled until the temperature of the solution reached 90 °C. Then, 1 mL of a HAuCl<sub>4</sub> solution (25 mM) was injected. After 30 min, the reaction was finished. This process was repeated twice. After that, the sample was diluted by extracting 55 mL of sample and adding 53 mL of MQ water and 2 mL of 60 mM sodium citrate. This solution was then used as a seed solution, and the process was repeated again. By changing the volume extracted in each growth step, it is possible to tune the seed particle concentration.

CLPFFD and isomers were synthesized by solid-phase synthesis using the 9-fluorenylmethoxycarbonyl/tert-butyl (Fmoc/tBu) strategy and a Multiple Advanced Chemtech 496 Synthesizer. Rink amide resin, N $\alpha$ -Fmoc-protected amino acids (4 equiv)/HBTU(4 equiv)/HOBt(4 equiv) and DIEA(8 equiv) were used. Fmoc protecting group was cleaved by treatment with a solution of 25% piperidine in DMF. Peptides were cleaved from the resin by treatment with 95% TFA, 2.5% TIS, 2.5% water for 2 h. C(VRLPPP)<sub>3</sub>, was synthesized manually by solid-phase synthesis using the 9-fluorenylmethoxycarbonyl/tert-butyl (Fmoc/tBu) strategy. 2-Chlorotrityl resin, N $\alpha$ -Fmoc-protected amino acids (2 equiv)/TBTU(2 equiv) and DIEA(6 equiv) were used. As a protecting group for the Arg side-chain, 2,2,4,6,7-pentamethyldihydrobenzofurane-5-sulfonyl (Pbf) was used. The Fmoc protecting group was cleaved by treatment with a solution of 20% piperidine in DMF (2 × 10 min). To incorporate the Fmoc-Arg(Pbf)-OH, the TBTU was replaced by PyBOP (2 equiv). C-SAP was cleaved from the resin by treatment with 95% TFA, 2.5% TIS, 2.5% water for 1 h 30 min. All peptides were purified by semipreparative RP-HPLC and characterized by MALDI-TOF mass spectrometry.

### 2.4 Gold Nanoparticles Conjugation

An aqueous peptide solution (20 μM) was added to the Au NP solution and stirred for 30 min at room temperature. Excess peptides were removed from the NPs by dialysis (3500 or 6-8000 MWCO depending on the sequence, Spectrum Lab, Rancho Dominguez, CA) for 3 days at room temperature. BSA degradation and reduction: BSA (Cohn Fraction V, Fluka) was degraded with trypsin (trypsin from bovine pancreas, E.C. 3.4.21.4, Roche).

BSA was incubated at 37 °C dissolved in Tris-HCl 100 mM at 150 μM, and trypsin was added at the final concentration of 35.8 mg/mL (3.94 U/mL, U: Chromozym Try as a substrate). After 24 h at 37 °C, tris(2-carboxyethyl) phosphine hydrochloride (TCEP) obtained from Fluka at a final concentration of 10.5 mM was added and incubated during 1 h 30 min at room temperature to reduce disulfide bonds. This solution was conjugated to Au NP with the same protocol used for the different peptides.

## 2.5 Cell Culture

Primary cultures of bone-marrow-derived macrophages were obtained from BALB/c mice (Harlan Ibérica, Barcelona, Spain) and cultured as previously described during 6 days at 37 °C and 5% CO<sub>2</sub> incubators in DMEM (BioWhittaker-Cambrex, Emerainville, France), supplemented with 20% FCS and 30% L-cell conditioned media. The use of animals was approved by the Animal Research Committee of the University of Barcelona (No. 2523). To render macrophages quiescent, they were deprived of M-CSF for 18 h before stimulation.

## 2.6 Proliferation Assay

After 24 h of treatment, cells were pulsed with 3H-dThd (1 µCi/mL) (Amersham Pharmacia Biotech, Piscataway, NJ) for 6 h as previously described. After stimulation, cells were fixed with MeOH 70% at 4 °C overnight. Then, three washes of TCA 10% were performed and cells were lysed with NaOH plus SDS. 3H incorporation was measured by standard liquid scintillation. Each point was performed in triplicate and the results were expressed as the mean ± SD.

## 2.7 Real-Time PCR

RNA Extraction and Real-Time PCR: Total RNA was extracted with the RNA Kit EZ-RNA (Biological Industries, Kibbutz beit hemeek, Israel) as indicated. cDNA was obtained from 1 µg of total RNA using M-MLV Reverse Transcriptase (Promega, Madison, WI) as described. Primer Express software (Applied Biosystems) was used to design primer sequences used for TNF-α, IL-1β, IL-6, and NOS2. Specific primer pairs were CCTGTGCTCCTCCTCTTTT GC and TCAGTGATGTAGCGACAGCCTG for TNF-α, CCTGTGTTTTCTCCTTGCCT and GCCTAATGTCCCCTTGAATCAA for IL-1β, CAGAAGGAGTGGCTAAGGACCA and ACGCACT AGGTTTGCCGAGTAG for IL-6, GCCACCAACAATGGCAACA and GTACCGGATGAGCTGTG AATT for NOS2, ACTATTGGCAACGAGCGGTTT and AAGGAAGGCTGGAAAAGAGCC for β-actin, forward and reverse, respectively. Thermal cycling conditions were 94 °C, 30 s; 60 °C, 30 s; 72 °C, 30s for 35 cycles. Each sample was analyzed in triplicate. Expression levels were normalized to β-actin. Relative values from a representative experiment out of two independent experiments are shown.

## 2.8 TEM Preparation

Cells were fixed with a glutaraldehyde 2.5% solution in PB 0.1 M for 1 h. After that cells were scraped, centrifuged at 4 °C, 2500 rpm, 10 min, and washed with PB 0.1 M. After the staining with OsO<sub>4</sub> 1% for 1 h, cells were dehydrated in acetone at 4 °C and infiltrated in Spurr epoxy resin. After embedment (60 °C, 48 h), 50 nm ultrathin sections were created with an ultramicrothom. Finally cells were stained with uranyl acetate and lead citrate.

# 3. RESULTS

## 3.1 Synthesis and Characterization of Gold Nanoparticles: Size and Shape Control.

Beyond the direct size-effect on immune response, the study of the interactions between Au NPs and immune system requires a wide catalog of NPs with controlled size, morphology, structure and composition. Thus, the increase of Au NP size (which entails a decrease of the curvature radii) increases the density number of loaded molecules<sup>18</sup>, therefore leading to different molecular ordering. As a result, a wide variety of Au NP conjugates, with different order, structure and density may be achieved by controlling Au NPs. Additionally, larger Au NPs show faceted crystals displaying flat surfaces, edges and corners.

Au NPs (~3 10<sup>12</sup> NPs/mL) of ~10 nm in diameter were prepared by injecting an aqueous HAuCl<sub>4</sub> precursor solution into a boiling solution of sodium citrate (SC). The role of sodium citrate (SC) in the formation and growing mechanism of Au NPs was systematically examined, obtaining that oxidation of SC can be induced either by the presence of HAuCl<sub>4</sub> or by its thermal decomposition under air<sup>16</sup>. As a result, it was proved that it is possible to increase the oxidation rate of SC by exchanging the order of reagent addition, which leads to a better control of Au NPs size and morphology in comparison to standard Turkevich approach. Size and morphology control of larger particles was achieved by developing a kinetically-controlled seeded-growth method in which the above synthesized 10 nm Au NPs were used as seeds<sup>15</sup>. The method focuses on the inhibition of secondary nucleation during the homogeneous growth process, while keeping the solution supersaturated enough to achieve the growth of seed particles via the catalyzed reduction of Au<sup>3+</sup> by sodium

citrate. The success of the method relies on the kinetic control of the growth process by adjusting reaction conditions, in particular, i) temperature, ii) pH level, and iii) seed concentration. As the kinetics of the gold reduction significantly depends on the temperature<sup>15</sup>, it is expected the decrease of the nucleation rate at lower temperatures (90°C), which leads to more favorable conditions for particle growth (kinetic control). Another important aspect is the pH of the solution, which has to be maintained around 7 during whole growth process<sup>19</sup> to control the reactivity of the Au<sup>3+</sup> species and avoid the protonation of citrate. This condition was achieved by adjusting the amount of SC on each growth step, using it as pH buffer. Finally, secondary nucleation of particles was avoided by both decreasing the temperature of the solution and carefully controlling the ratio between gold precursor added and concentration of seed particles. The control of all of these parameters allows not only the synthesis of monodisperse Au NPs with diameters ranging from 10 to 200 nm but also provides key aspects, identifying and explaining the important synthetic variables that must be controlled in order to control the Au NP morphology.

Figure 1-A shows morphological characterization of resultant Au NPs obtained by Transmission Electron Microscopy (TEM), where it can be seen how the final size of the particles increases (from 10 to 150) as the number of growth steps increases (from 1 to 13). As each growth step withstand the dilution of previously obtained particles, the concentration of the colloidal solutions depends on particle size ranging from  $\sim 3 \cdot 10^{12}$  NP/mL (10 nm) to  $\sim 8 \cdot 10^9$  NP/mL (150 nm). It is important to note here that, although the particles are rather faceted and thus not perfectly spherical, the growth is very uniform, without the formation of elongated particles or a second population of smaller particles. A detailed description of the process has been previously published by our group<sup>15</sup>.

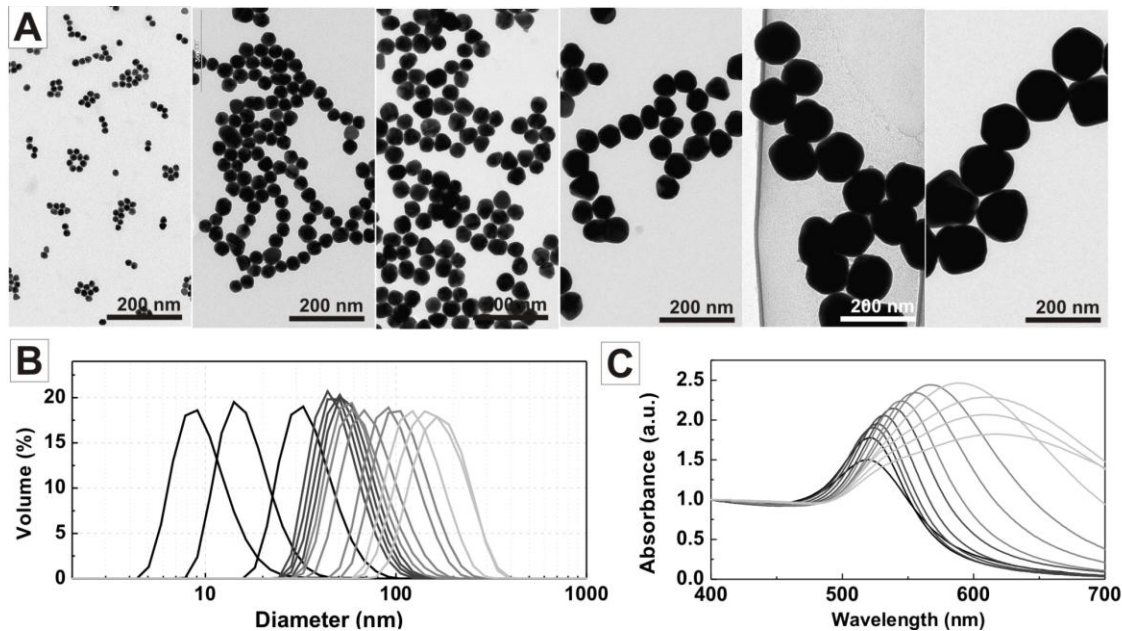


**Figure 1.** Kinetically-controlled Seeded-growth of citrate-stabilized gold nanoparticles the seed solution. (A) Transmission electron microscopy images of Au NPs obtained after different growth steps. From left to right:  $\sim 18$  nm (1st GS);  $\sim 30$  nm (3rd GS),  $\sim 42$  nm (5th GS);  $\sim 70$  nm (6th GS);  $\sim 110$  nm (11th GS) and  $\sim 150$  nm (13th GS). (B) Hydrodynamic size distribution of synthesized Au NPs measured by Dynamic Light Scattering. Mean size increases from  $\sim 8.5$  nm (seed particles) up to 165 nm after 13th growth steps. (C) UV-vis spectra of Au colloids obtained after different growth steps. All spectra all normalized at 400 nm to facilitate comparison.

To further corroborate sample uniformity, size distribution of colloidal solutions was studied by Dynamic Light Scattering (DLS). Figure 1-B shows DLS distributions of Au NPs synthesized after different growth steps, obtaining that hydrodynamic size increases from  $\sim 8.5$  nm, in the case of seed particles, up to  $\sim 165$  nm, after 13 growth steps. Moreover, distributions are monomodal, which indicates that neither secondary nucleation nor aggregation of Au NPs occurred during the growth process. The optical properties of Au NP solutions were measured by UV-Vis spectroscopy (Fig. 1-C).

An initial red-shift, from 518.5 to 556 nm of the surface plasmon resonant (SPR) band, indicative of the mean size distribution of the colloidal gold solution, was obtained as the size of Au NPs increased from ~ 8.5 nm to ~ 95 nm . Further increase of Au NP size leads to a broadening of the main dipolar resonance band, peaking at ~ 575 nm for Au NPs with an average diameter of ~110 nm. Interestingly, above 120 nm, the single band is accompanied by a shoulder at lower wavelengths, corresponding to a quadrupolar resonance, placed at ~540 nm for 150 nm Au NPs<sup>20</sup>. These experimental absorbance data are in fully agreement with performed calculations based on the standard Mie theory of spherical particles<sup>15</sup>.

### 3.2 Functionalization of Gold Nanoparticles with Peptides

As a model for our work, four biomedical significant peptides were conjugated to ~ 10 nm Au NPs: i) Amyloid Growth Inhibitor peptide –CLPFFD-NH<sub>2</sub>–, comprising amino acids 11 to 16 from the Aβ<sub>1-42</sub> protein that recognize a particular hydrophobic domain of the β-sheet structure<sup>21</sup> and ii) Sweet Arrow Peptide –C(VRLPPP)<sub>3</sub>–, a non-toxic cell-penetrating peptide intended for intracellular drug delivery<sup>22</sup> and iii) two isomers of CLPFFD-NH<sub>2</sub> peptide, (CLPDDF-NH<sub>2</sub> and CDLPFF-NH<sub>2</sub>). All the peptides used in our studies present a thiol group in the side chain of the N-terminal cysteine (C) which is able to make a covalent bond to the gold surface<sup>23</sup>. This interaction may be additive to that of the N-terminal primary amine, since amino groups are also known to have a strong interaction with gold surfaces<sup>24</sup>. Moreover, it has been shown that the presence of a positively charged amino group in the vicinity of the thiol significantly accelerates the adsorption kinetics of thiols onto citrate-stabilized Au NPs<sup>25</sup>. The isoelectric point of aminoacids and peptides was studied (Figure 2), obtaining that, at physiological pH, CLPFFD-NH<sub>2</sub>, CLPDDF-NH<sub>2</sub> and CDLPFF-NH<sub>2</sub> presents one negative charge while C(VRLPPP)<sub>3</sub>-COOH presents three positives charges. In these cases, when the peptide is linear and the terminal aminoacid is highly hydrophilic, water is excluded and a dense self-assembled monolayer is formed at Au NP surface leading to homogeneous conjugates.

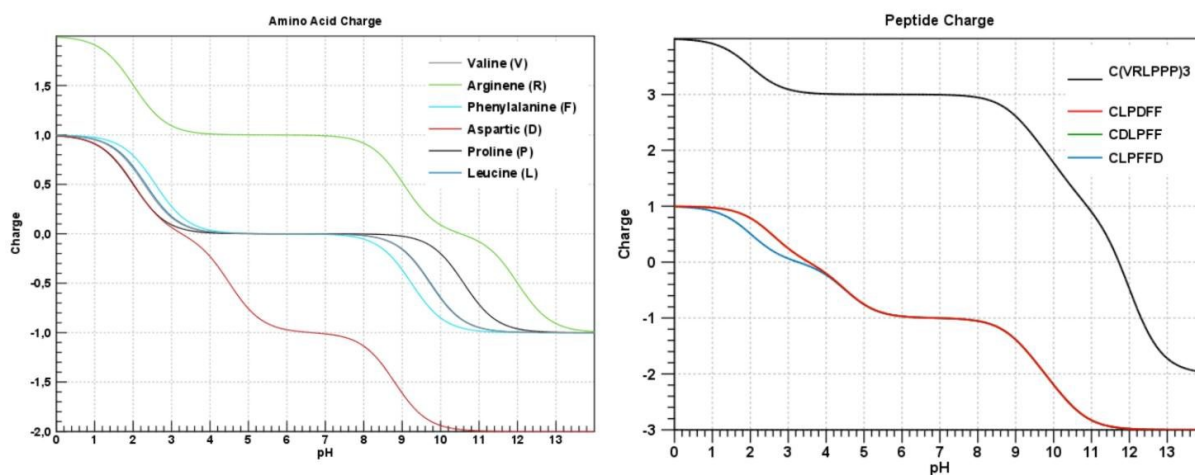


**Figure 2.** Amino acid (Left) and peptide (Right) charge as a function of the pH of the solution.

As conjugation of one peptide generates a homogenous distribution of peptides onto Au NP surface, we attempt to produce heterogeneous Au NP conjugates. Thus, two peptides of different size, C-LPFFD-NH<sub>2</sub> and C-(VRLPPP)<sub>3</sub>-COOH, or three peptides of different polarity, C-LPFFD-NH<sub>2</sub>, C-LPDDF-NH<sub>2</sub>, and C-DLPFF-NH<sub>2</sub>, were coupled to Au NP as their mixtures (AuNP-2PEP, AuNP-3PEP, respectively). Bovine Serum Albumin (BSA) fragments and Fetal Calf Serum (FCS) proteins, which are present on cell culture media (FCS enriched DMEM, [FCS:DMEM]=1:10), were also conjugated to the Au NPs as controls of heterogeneous conjugates.

The conjugation process was performed incubating Au NPs with an excess of the N-terminal cysteine peptide (20 μM) in an aqueous solution for 30 min. The conjugation was carried out in the presence of an excess of peptide in order to ensure full coverage of Au NPs, obtaining therefore an homogeneous conjugation. In order to remove the excess of unbound peptide, all samples were purified by dialysis. Conjugates were characterized by UV-Vis spectroscopy,

$\zeta$ -Potential and Dynamic Light Scattering. Citrate-stabilized Au NPs are stable in water and display a characteristic UV-Vis absorption spectrum with a plasmon band peaking at  $\sim 518$  nm. The absorption spectrum is sensitive to Au NP environment and an observable red-shift of about 8-10 nm can be observed once peptides, CLPFFD-NH<sub>2</sub> and C(VRLPPP)<sub>3</sub>-COOH, are attached. The shift occurs in a few seconds, suggesting that conjugation process is fast, and spectra are then stable for weeks. Peptide-conjugation process was also monitored by DLS and  $\zeta$ -Potential measurements. The increases in the hydrodynamic size of the NPs as well as drop in the surface charge once the peptides are conjugated to Au NPs, confirm the conjugation process<sup>8,26</sup>. Similarly, the conjugation of Au NPs to CLPDDF-NH<sub>2</sub> and CDLPFF-NH<sub>2</sub>, which contain the same amino acids as CLPFFD albeit in a different sequence, was followed by UVVis spectroscopy, DLS and  $\zeta$ -potential measurements. In this case, SPR red-shifts from 518 nm (Au NPs) to 526 nm (AuNP-CDLPFF-NH<sub>2</sub>) and to 524.5 nm (AuNP-CLPDDF-NH<sub>2</sub>) were observed and DLS measurements showed an increase of the hydrodynamic diameter of approximately 5 nm, once CLPDDF-NH<sub>2</sub> and CDLPFF-NH<sub>2</sub> are attached to Au NP surface.  $\zeta$ -potential results suggest not only the success of the conjugation process but also that these conjugates are stable by mainly by steric means.

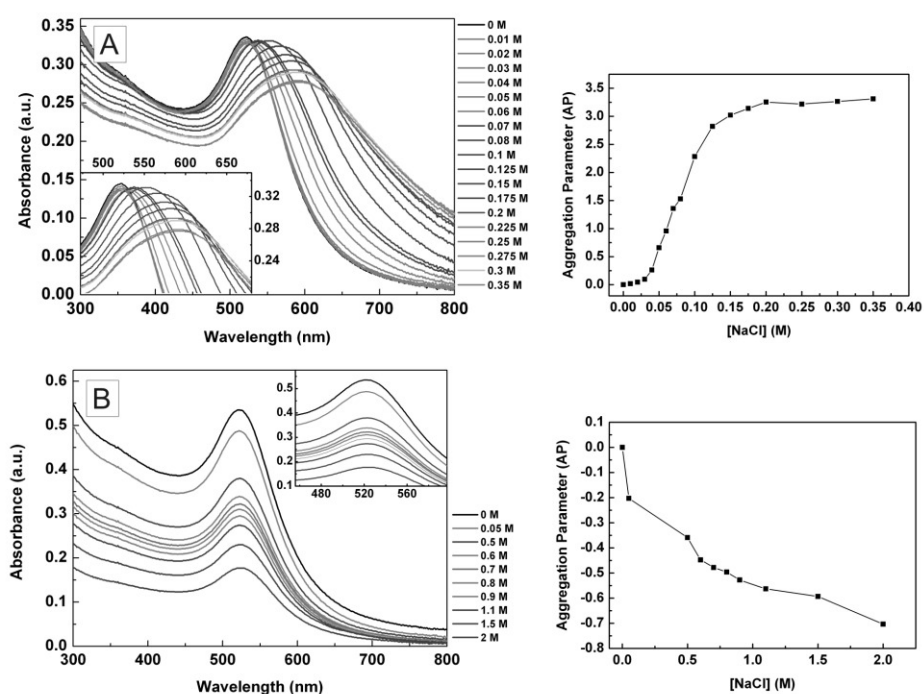


**Figure 3.** Effect of ionic strength on the stability of citrate-stabilized Au NPs and CLPFFD-conjugated Au NPs. UV-Vis absorption spectra of Au NPs (A) and CLPFFD-conjugated Au NPs (B) at pH 7 in the presence of an added amount of NaCl, and Aggregation parameters as a function of [NaCl]. The quantities refer to concentrations in the final solution. The decrease of the overall spectra in the case of CLPFFD-conjugated Au NPs is a consequence of the sample dilution that took place when the NaCl solution was added.

Colloidal particles have an inherent tendency to aggregate due to attractive van der Waals (vdW) forces. In order to stabilize the particles against these attractive forces, it is necessary to introduce a repulsive inter-particle force, either by electrostatic or a steric means. In the case of Au NPs, typically synthesized following a sodium-citrate reduction reaction, their electrostatic stabilization arises from a mutual repulsion that occurs as a result of the negative surface of the citrate Au NP coating. Oppositely, in the case of Au NPs conjugates the stabilization mechanism can be provided either by electrostatic, steric or electro-steric interaction. Steric interactions of a molecule with a surface layer can

provide greater stability to a colloid than pure electrostatic interactions, since the latter is very sensitive to the pH and the ionic strength of the solution<sup>27</sup>.

Almost for any application, specially biomedicine, the colloidal stability is a necessity. In order to evaluate the stabilization mechanism and robustness of Au NP and their conjugates, we studied the aggregation rate of the colloidal solution against changes in the ionic strength of the medium, by monitoring the absorption spectra of Au NPs. It is stated that aggregation processes are concomitant with a red-shift and broadening of SPR band, due to dipole coupling between the plasmons of neighboring particles<sup>28,29</sup>. In fact, this aggregation can be quantified by the increase of the aggregation parameter<sup>30</sup>, which measures the variation of the integrated absorbance between 600 and 700 nm<sup>30-32</sup>. Figure 3 shows a set of UV-Vis spectra of citrate-stabilized Au NPs and peptide-conjugated Au NPs at various ionic strengths values taken 15 min after the addition of different amounts of sodium chloride (NaCl), where it can be seen how citrate-stabilized Au NPs agglomerate more and more as the amount of NaCl increases. On the contrary, no virtual changes in the position of the SPR can be detected in the case of peptide-conjugated Au NPs. From these results can be concluded that the stability of Au NPs conjugates is determined by the stabilization mechanism. Thus, electrically stabilized citrate-coated Au NPs, are prompt to precipitate by changing the ionic strength of the medium while Au NPs conjugates, stabilized by the interactions of molecules side chains or domain, are stable in a broad range of ionic strengths and pH.

### 3.3 Addressing The Immune System: Macrophages Response towards Peptide-Conjugated Gold Nanoparticles

The ability of Au NP and peptidic conjugates to activate the immune system was tested using mice bone marrow macrophages as an in vitro model of primary culture of macrophages<sup>33</sup>. Macrophage proliferation is a well established method to verify macrophage activation. Thus, in vitro exposition of macrophages to pathogens and microbe substances involves a blockage of proliferation and the acquisition of effector functions<sup>34,35</sup> producing pro-inflammatory cytokines, such as TNF- $\alpha$ , IL- $\beta$  and IL-6 as well as the induction of nitric oxide synthase (NOS2)<sup>36</sup>.

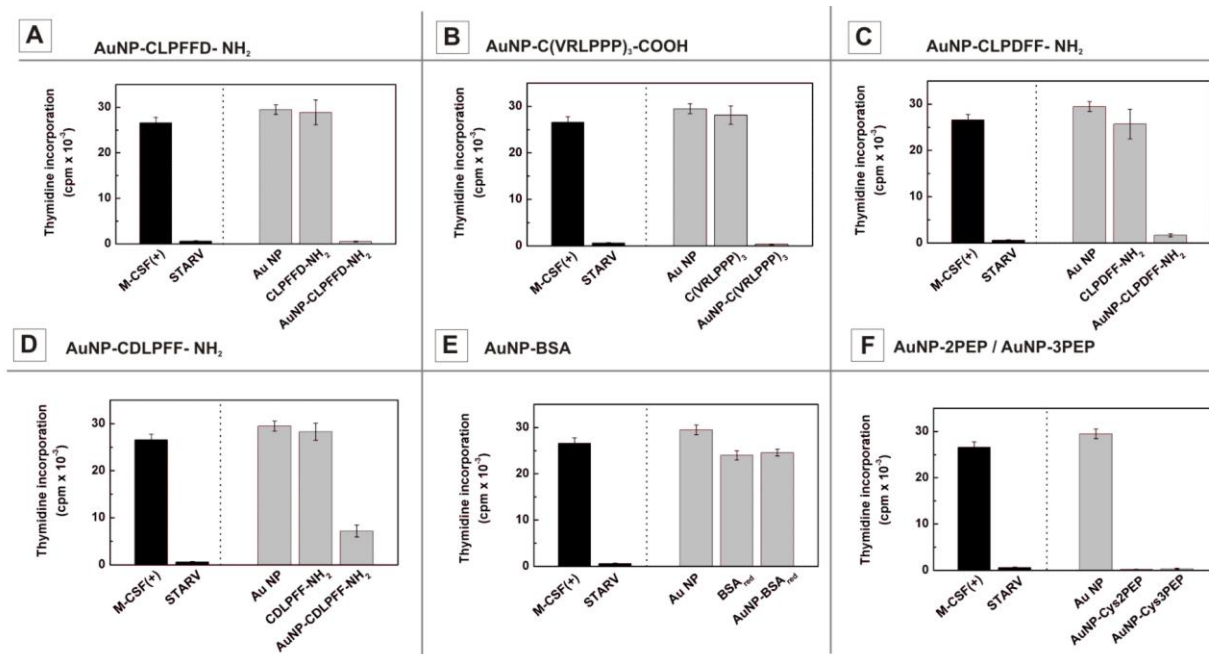


**Figure 4.** Macrophage thymidine incorporation assay of Au NP, peptides and conjugates. A) AuNP-CLPFFD-NH<sub>2</sub> and controls, B) AuNP-C(VRLPPP)<sub>3</sub>-COOH and controls, C) AuNP-CLPDDFF-NH<sub>2</sub> and controls, D) AuNP-CDLPPFF-NH<sub>2</sub> and control, E) AuNP-BSA and controls and F) AuNP-2PEP / AuNP-3PEP and controls. Resting macrophages were stimulated with 1200 U/ml of M-CSF in the presence of the indicated substances (1 $\mu$ M). After 24 hours, thymidine incorporation was measured. Similar results were found in all cases, the peptide-conjugated Au NPs inhibited the macrophage proliferation while the peptides, Au NPs or AuNP-BSA conjugates did not.



The potential pro-inflammatory response of macrophages towards Au NPs conjugates and controls were studied analyzing both cytokines production and macrophage proliferation. Macrophage proliferation was assessed by radioactive thymidine incorporation. Results plotted in Figure 4 indicate that macrophage proliferation was not affected either by citrate-stabilized Au NP or free peptides whereas the corresponding conjugates completely blocked proliferation in a dose dependent manner (Fig. 4A-D). Interestingly, the mixture of two peptides of different size (AuNP-2PEP) or three peptides of different polarity (AuNP-3PEP) managed to block macrophage proliferation (Fig. 4F). Since no methodology was available to assess peptide homogeneity on the Au NP surface, we were unable to discern the resulting degree of disorganization. Furthermore, homogeneity could be maintained since conjugation kinetics for each peptide are likely to be different, thereby leading to ordered peptide domains on the surface of the Au NP. In this regard, several reports have shown how different molecules segregate and form defined domains on the surface of NPs<sup>37,38</sup>. On the contrary, Au NPs functionalized with BSA fragments were not able to block macrophage proliferation (Fig. 4E). Moreover, the simultaneous addition of citrate-stabilized Au NP and CLPFFD-NH<sub>2</sub> to the cell culture did not block macrophage proliferation, suggesting that self-conjugation has not occurred because the ability of Au NP to attach to CLPFFD-NH<sub>2</sub> is quenched by proteins present in the medium<sup>39,40</sup>. In this context, blockage of macrophage proliferation seems to be, to some extent, independent on peptide size, charge and composition, but not on coating order.

The potential pro-inflammatory response of macrophages to Au NP conjugates and controls was studied by analyzing the induction of cytokines (TNF- $\alpha$ , IL- $\beta$  and IL-6) as well as nitric oxide synthase (NOS2). LPS was used at subsaturant concentrations as a positive control. Accordingly with proliferation arrest, results showed in Figure 5 prove that neither peptides nor citrate-stabilized Au NPs activated any pro-inflammatory response since both the cytokines and NOS2 levels were similar to the untreated starved control. However, an exacerbated cytokine and nitric oxide synthase induction was observed in the case of peptide-conjugated Au NPs, indicating a classical macrophage pro-inflammatory response.

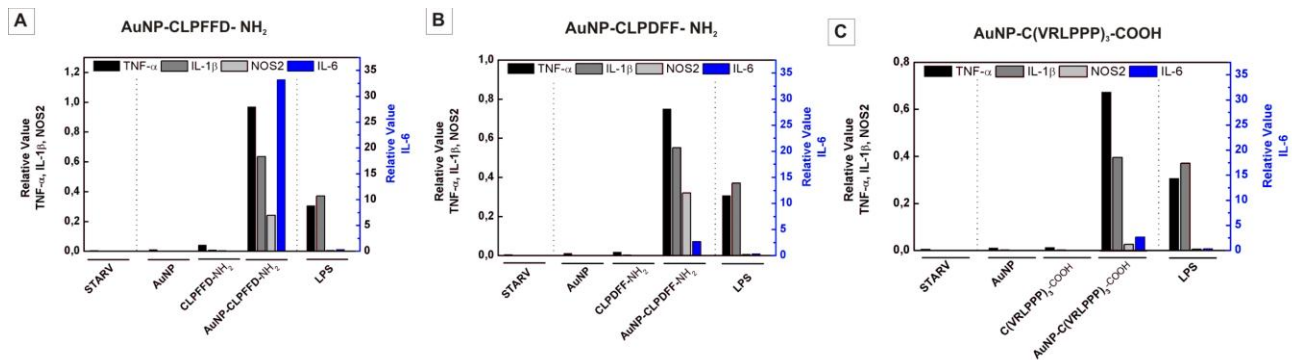


**Figure 5.** Peptides conjugated Au NPs induced a pro-inflammatory response in macrophages as can be measured by Real Time PCR. (A) CLPFFD-NH<sub>2</sub> and their conjugates, (B) CLPDFF-NH<sub>2</sub> and their conjugates and (C) (VRLPPP)<sub>3</sub>-COOH and their conjugates. mRNA levels of TNF- $\alpha$ , IL-1 $\beta$ , IL-6 and NOS2 are measured in relation to  $\beta$ -actin of macrophages stimulated for 6 hours with LPS (10 ng/ml) or with the indicated substances (1  $\mu$ M) in the presence of M-CSF.

To verify that conjugate effects on macrophage proliferation were specific and not a reflection of cell death, apoptosis assays were carried out by flow cytometry using Annexin V, as apoptosis marker, in combination with Propidium Iodide (PI). Obtained results (data not shown) indicated that none of the substances used in this study compromised cell viability, indicating that their effects on proliferation were specific, and suggesting the possibility to induce macrophage activation by peptide-conjugated Au NPs, without causing nor altering their cell viability.

Since the blockage of macrophage proliferation and production of cytokines withstand the engagement of phagocytosis, we investigated the response and phagocytic activity of macrophages in the presence of Au NP conjugates by TEM.

Results depicted in Figure 6 reveal an early (15 min) internalization of peptide-conjugated Au NPs, with the highest number of particles internalized after 6 hours, and virtually no particles after 12 hours. Oppositely, the incubation of macrophages with non-conjugated Au NPs, or BSA-digest coated Au NPs, revealed no internalization at any time even after exhaustive TEM observation.

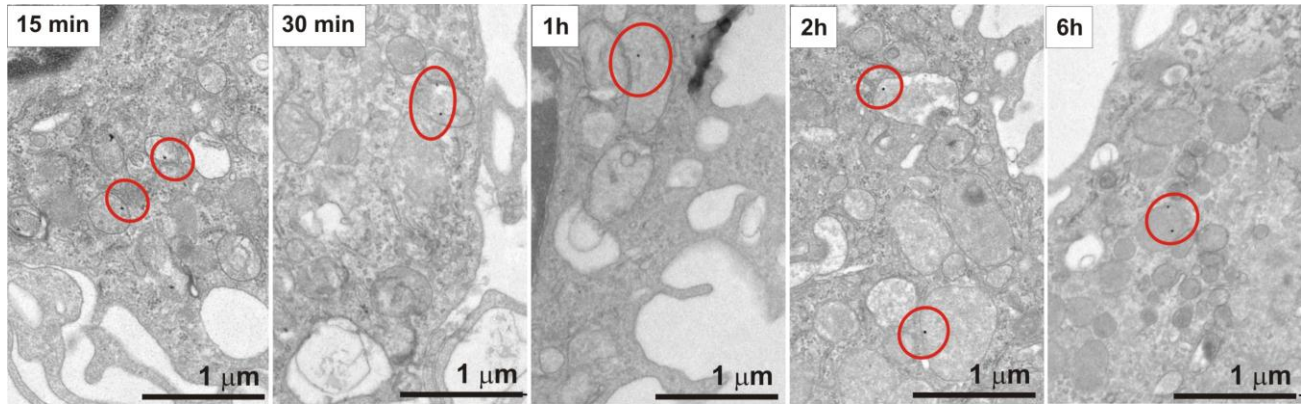


**Figure 6.** Internalization of Au NPs Conjugates observed by Transmission Electron Microscopy (TEM). Representative resin-tomography images revealing internalization of AuNP-CLPFFD-NH<sub>2</sub> at 15 min, 30 min, 1 h, 2 h and 6 h.

## 4. DISCUSSION AND CONCLUSIONS

### 4.1 The Effect of the Order in the Peptide Layer

Recently, it has emerged a clear relationship between protein quaternary structure and higher order organization with immunogenicity<sup>41,42</sup>. Not surprisingly, many viruses exhibit a quasi-crystalline, highly organized surface that displays a regular array of epitopes. In addition, the presentation of an antigen in a highly ordered and repetitive array has proved to provoke strong antibody responses in mice, whereas the same antigen presented as a monomer is non-immunogenic<sup>43-46</sup>. Following these principles it has been observed that the display of peptides, proteins or antigens in an ordered, repetitive array (epitope repetition)<sup>43</sup> are known to induce an enhanced immune response relative to vaccination with the "free" protein antigen<sup>4</sup>. This phenomenon is also observed in bacterial surfaces, virus-like particles (VLPs) and those formed on certain viral proteins<sup>47,48</sup>. Similarly, surface derivation of liposome drug carriers avoid the elimination by macrophages (mainly PEGylation) which results in an increase in the blood circulating times<sup>49</sup>. Virus-like particles (VLPs) consist of viral structural proteins that, when over-expressed, spontaneously self-assemble into particles that are antigenically indistinguishable from infectious virus or subviral particles. However, proteins that spontaneously assemble to highly repetitive structures, such as VLPs, are rare exceptions. Therefore, epitope-specific antibody responses may be induced by VLPs that contain peptides inserted in their immunodominant regions. However, due to steric problems, the size of the peptides capable of being incorporated into VLPs while still permitting capsid assembly is rather limited. In this sense, NPs have been recently used to electrostatically assist the assembly of bromovirus mosaic virus coating preserving virus size, structure and physico-chemical properties of the native virus<sup>50</sup>. However, this electrostatic bonding needs an excess of conjugating protein in order to be stable and in equilibrium, and may lose stability *in vivo*.

Taking into account the above mentioned observations, it can be concluded that the condition for macrophage activation is related to the ordered display of peptides, proteins or antigens. Therefore, in our studies we used Au NPs as scaffolds to force the self-assembly of peptides onto Au surface. Moreover, the nature of the peptide chain allows the control of packaging degree which determines immune response. In this context, the different immune response obtained for

CLPFFD-NH<sub>2</sub> and its isomers CLPDDF-NH<sub>2</sub> and CDLPFF-NH<sub>2</sub> can be explained regarding the different degree of conjugation. Amino acids L, P and F are hydrophobic and only the amino acid D presents a negative charge at physiological pH, while C is neutral. Thus, the position of the negative charge could be related with the degree of conjugation of each peptide on the surface of the Au NP. In the case of CLPFFD-NH<sub>2</sub>, when the peptide adopts an extended conformation, the D residue localizes away from the gold surface and leads to a higher degree of packing<sup>51</sup>. However, when the D residue is near the Au NP surface (AuNP-CDLPFF-NH<sub>2</sub>), a higher repulsion between D residues and the exposure of the hydrophobic residues, leads to a lower degree of packing. In the case of CLPDDF-NH<sub>2</sub>, an intermediate situation occurs. Therefore, the degree of conjugation is AuNP-CLPFFDNH<sub>2</sub> > AuNP-CLPDDF-NH<sub>2</sub> > AuNP-CDLPFF-NH<sub>2</sub> which is consistent with the observed degree of proliferation arrest (Fig.3). These results were confirmed by circular dichroism<sup>52</sup> and amino acid analysis. Similarly, the blockage of macrophage immune response towards AuNP- C(VRPPP)<sub>3</sub> -COOH can be explained in terms of the highly packed layers formed by the C(VRPPP)<sub>3</sub> -COOH at Au NP surface. In addition, neither the conjugation of Au NPs to BSA fragments nor the non-specific conjugation of Au NPs to media proteins produce activation of macrophage immune response. In this context, it is possible to conclude that the condition for the activation of macrophage response is related to the homogeneity of the peptide coating layer. In a similar set of experiments, a different immune response was obtained. Using the same conjugates on other in vitro differentiated macrophages, the cells apparently detected the Au NPs, but did not elicit any proinflammatory reaction (absence of cytokine induction or proliferation arrest) while showing massive internalization of the NPs (Fig.7), suggesting a tolerant response. More analysis on this response will try to correlate structure with degree and type of immune response.

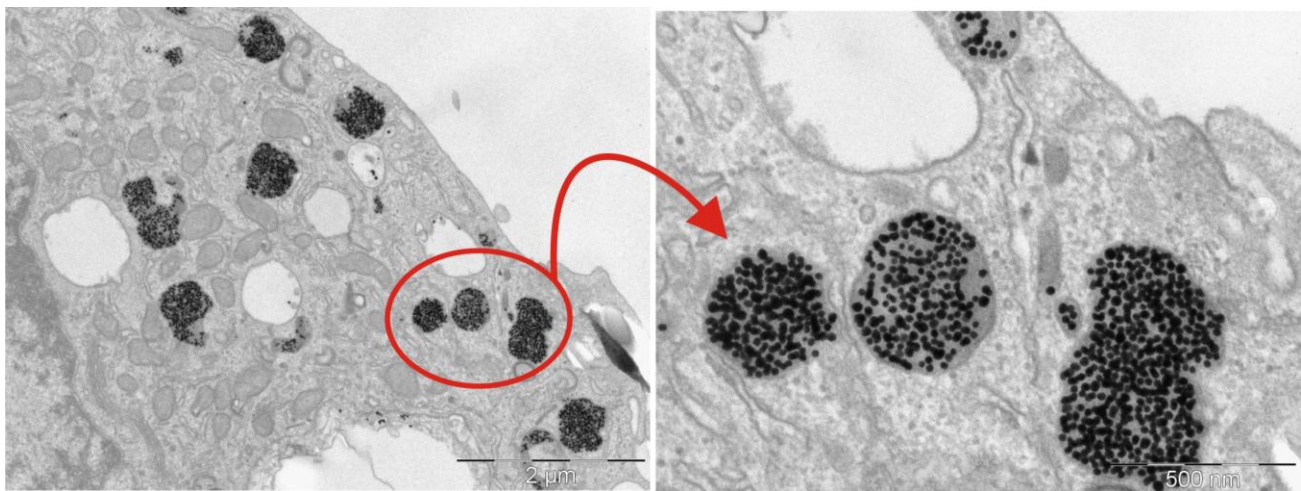


**Figure 7.** Massive Internalization of Au NPs Conjugates observed by Transmission Electron Microscopy (TEM). Representative resin-tomography images revealing massive internalization of AuNP-CLPFFD-NH<sub>2</sub> after 1 hour of exposition.

#### 4.2 Immunomodulatory Properties of Peptide-functionalized Gold Nanoparticles

Several conclusions can be drawn from this set of experiments. First, the establishment of a simple set of conditions whereby Au NP conjugates can escape from the immune barrier, based upon the design or disorder of a coating structure that is very feasible. It is especially important to note that the final biological entity is the one resulting from the interaction of the NP conjugates and the proteins in serum medium<sup>53</sup>, which is size and time<sup>39</sup> and composition dependent<sup>40</sup>. Second, the controlled activation of macrophages (and similar effects found in monocytes and dendritic cells) may generate adjuvant activity for use in vaccines. The induction of antibodies by prophylactic vaccination against infectious diseases has been the most effective medical intervention in human history. The greatest concern regards immediate hypersensitivity responses that cause anaphylactic responses. Such responses have been most commonly

observed in treatment with bacterial products such as asparaginase, streptokinase, and diphtheria toxin-conjugated molecules. Although inactivated or attenuated vaccines are relatively safe, there is nevertheless a certain probability that pathogens might revert to a virulent phenotype *in vivo* and cause disease, as it is sometimes observed after vaccination against polio virus. Consequently, modern vaccines are usually produced recombinantly and do not replicate in the host. Unfortunately, isolated soluble components of viruses and other pathogens are often poorly immunogenic in the absence of non-specific inflammatory stimuli<sup>54</sup>.

Recombinant vaccines therefore need to be administered together with an adjuvant to enhance immunogenicity. However, effective adjuvants are not well tolerated, and only a few of them have the potential to be used in human subjects. When looking for alternatives, we observed how the order of NP surface molecules, rather than its chemical composition or agglomeration state, is crucial in determining the interaction of NPs with the immune system. Thus, tools to improve antigen presentation to the immune system based on the conjugation of inorganic NPs to peptides and the rational design of their peptide coating may provide a useful toolkit for vaccinologists and may also serve to change and modulate immune response in the fight against allergies, rejection, cancer and autoimmune diseases. In general, it has been shown that by providing a TRL ligand with vaccine, the immune response can be both stronger and more profound. In particular, Structure Activity Relationship studies (as well as those addressing adjuvant-antigen conjugation) have shown that ligand modification can alter the magnitude and character of immune activation, therefore demonstrating that structural modification of adjuvants may be therapeutically beneficial. In this scenario, the use of Au NPs conjugates as adjuvants may offer several natural advantages: rational design, low toxicity, low-cost and modifiable biodistribution<sup>27</sup> (molecules bound to NPs travel in a different way through the body than those that are unbound). Additionally, Au NPs can be loaded with different complementary molecules, or combinations of adjuvants and antigens. These higher-ordered structures might facilitate TLR cross-linking and promote the recruitment of one or more additional cofactors or adaptor proteins to the signaling complex. Finally, conjugation of antigens to Au NPs can modify the antigen delivery mechanism and other immunogenic properties. There is promising evidence that these strategies (i.e., conjugation of adjuvants, cofactors, and adaptors with antigens) are effective. All of these advances will provide immunologists with an entirely new toolbox with which they can tailor their specific approaches.

All of this points are relevant for the future development of NP-based medical devices which have to travel to distant organs avoiding elimination by the immune system before reaching their target (and avoiding inflammation). In addition two other aspects might be considered. First, conjugation protects against systemic degradation<sup>55</sup>. And second, NPs change biodistribution of its attached molecules in such a way that they are accumulated in highly phagocytosing organs as liver, spleen or in the lymph nodes where the adaptive immune response is mainly produced<sup>56</sup>. All in all, the response of the immune system towards nanostructured materials is not unique. Thus, some of them may induce a (pro)-inflammatory response being taken up by phagocytic cells, whereas others seem to reduce these activities reducing the ability of these immune cells to fight. Unfortunately, predicting the innate response (*in vitro* or *in vivo*) of NPs is still difficult to achieve.

## ACKNOWLEDGMENTS

The authors acknowledge financial support from the grants "Plan Nacional" from the Spanish Ministry of Science and Innovation (MAT2009-14734-C02-01) and "Nanotecnologías en biomedicina (NANOBIOMED)" from the Consolider-Ingenio 2010 Program (CSD2006-00012). N.G.B. thanks Spanish Government for financial support through the "Juan de la Cierva" program.

## REFERENCES

- (1) Bastús, N. G.; Casals, E.; Vazquez-Campos, S.; Puentes, V. *Nanotoxicology* **2008**, *2*, 99-112.
- (2) Sperling, R. A.; Parak, W. J. *Philosophical Transactions of the Royal Society A: Mathematical, Physical and Engineering Sciences* **2010**, *368*, 1333-1383.
- (3) Casals, E.; Vazquez-Campos, S.; Bastús, N. G.; Puentes, V. *Trac-Trends in Analytical Chemistry* **2008**, *27*, 672-683.
- (4) Turvey, S. E.; Hawn, T. R. *Clin Immunol* **2006**, *120*, 1-9.
- (5) Moghimi, S. M. *Biochimica et Biophysica Acta (BBA) - Molecular Cell Research* **2002**, *1590*, 131-139.
- (6) Ishida, T.; Kiwada, H. *International Journal of Pharmaceutics* **2008**, *354*, 56-62.
- (7) Wang, X.; Ishida, T.; Kiwada, H. *Journal of Controlled Release* **2007**, *119*, 236-244.
- (8) Bastús, N. G.; Sanchez-Tillo, E.; Pujals, S.; Farrera, C.; Lopez, C.; Giralt, E.; Celada, A.; Lloberas, J.; Puentes, V. *ACS Nano* **2009**, *3*, 1335-1344.
- (9) Kim, J. A.; Aberg, C.; Salvati, A.; Dawson, K. A. *Nat Nano* **2011**, *7*, 62-68.
- (10) Sperling, R. A.; Casals, E.; Comenge, J.; Bastús, N. G.; Puentes, V. F. *Current Drug Metabolism* **2009**, *10*, 895-904.
- (11) Dobrovolskaia, M. A.; McNeil, S. E. *Nat Nano* **2007**, *2*, 469-478.
- (12) Perrault, S. D.; Walkey, C.; Jennings, T.; Fischer, H. C.; Chan, W. C. W. *Nano Letters* **2009**, *9*, 1909-1915.
- (13) Kim, J. S.; Yoon, T.-J.; Yu, K. N.; Kim, B. G.; Park, S. J.; Kim, H. W.; Lee, K. H.; Park, S. B.; Lee, J.-K.; Cho, M. H. *Toxicological Sciences* **2006**, *89*, 338-347.
- (14) Fang, C.; Shi, B.; Pei, Y.-Y.; Hong, M.-H.; Wu, J.; Chen, H.-Z. *European Journal of Pharmaceutical Sciences* **2006**, *27*, 27-36.
- (15) Bastús, N. G.; Comenge, J.; Puentes, V. *Langmuir* **2011**, *27*, 11098-11105.
- (16) Ojea-Jimenez, I.; Bastús, N. G.; Puentes, V. *The Journal of Physical Chemistry C* **2011**, *115*, 15752-15757.
- (17) Ojea-Jimenez, I.; Romero, F. M.; Bastús, N. G.; Puentes, V. *Journal of Physical Chemistry C* **2010**, *114*, 1800-1804.
- (18) Hill, H. D.; Millstone, J. E.; Banholzer, M. J.; Mirkin, C. A. *ACS Nano* **2009**, *3*, 418-424.
- (19) Ji, X.; Song, X.; Li, J.; Bai, Y.; Yang, W.; Peng, X. *J. Am. Chem. Soc.* **2007**, *129*, 13939-13948.
- (20) Rodriguez-Fernandez, J.; Perez-Juste, J.; Garcia de Abajo, F. J.; Liz-Marzan, L. M. *Langmuir* **2006**, *22*, 7007-7010.
- (21) Kogan, M. J.; Bastús, N. G.; Amigo, R.; Grillo-Bosch, D.; Araya, E.; Turiel, A.; Labarta, A.; Giralt, E.; Puentes, V. F. *Nano Letters* **2006**, *6*, 110-115.
- (22) Pujals, S.; Bastús, N. G.; Pereiro, E.; Lopez-Iglesias, C.; Puentes, V. F.; Kogan, M. J.; Giralt, E. *ChemBiochem* **2009**, *10*, 1025-1031.
- (23) Sellers, H.; Ulman, A.; Shnidman, Y.; Eilers, J. E. *Journal of the American Chemical Society* **1993**, *115*, 9389-9401.
- (24) Zhang, J. D.; Chi, Q. J.; Nielsen, J. U.; Friis, E. P.; Andersen, J. E. T.; Ulstrup, J. *Langmuir* **2000**, *16*, 7229-7237.
- (25) Bellino, M. G.; Calvo, E. J.; Gordillo, G. *Physical Chemistry Chemical Physics* **2004**, *6*, 424-428.
- (26) Bastús, N. G.; Sanchez-Tillo, E.; Pujals, S.; Farrera, C.; Kogan, M. J.; Giralt, E.; Celada, A.; Lloberas, J.; Puentes, V. *Molecular Immunology* **2009**, *46*, 743-748.
- (27) Ojea-Jimenez, I.; Puentes, V. *Journal of the American Chemical Society* **2009**, *131*, 13320-13327.
- (28) Storhoff, J. J.; Lazarides, A. A.; Mucic, R. C.; Mirkin, C. A.; Letsinger, R. L.; Schatz, G. C. *Journal of the American Chemical Society* **2000**, *122*, 4640-4650.
- (29) Kreibitz, U. V., M. *New York, Springer* **1995**.
- (30) Levy, R.; Thanh, N. T. K.; Doty, R. C.; Hussain, I.; Nichols, R. J.; Schiffrin, D. J.; Brust, M.; Fernig, D. G. *J. Am. Chem. Soc.* **2004**, *126*, 10076-10084.
- (31) Weisbecker, C. S.; Merritt, M. V.; Whitesides, G. M. *Langmuir* **1996**, *12*, 3763-3772.

- (32) Sastry, M.; Lala, N.; Patil, V.; Chavan, S. P.; Chittiboyina, A. G. *Langmuir* **1998**, *14*, 4138-4142.
- (33) Celada, A.; Gray, P. W.; Rinderknecht, E.; Schreiber, R. D. *J Exp Med* **1984**, *160*, 55-74.
- (34) Vadiveloo, P. K. *Journal of Leukocyte Biology* **1999**, *66*, 579-582.
- (35) Xaus, J.; Comalada, M.; Valledor, A. F.; Cardo, M.; Herrero, C.; Soler, C.; Lloberas, J.; Celada, A. *Immunobiology* **2001**, *204*, 543-50.
- (36) Valledor, A. F.; Xaus, J.; Marques, L.; Celada, A. *Journal of Immunology* **1999**, *163*, 2452-2462.
- (37) Devries, G. A.; Brunnbauer, M.; Hu, Y.; Jackson, A. M.; Long, B.; Neltner, B. T.; Uzun, O.; Wunsch, B. H.; Stellacci, F. *Science* **2007**, *315*, 358-61.
- (38) Jackson, A. M.; Myerson, J. W.; Stellacci, F. *Nat Mater* **2004**, *3*, 330-6.
- (39) Casals, E.; Pfaller, T.; Duschl, A.; Oostingh, G. J.; Puentes, V. *ACS Nano* **2010**, *4*, 3623-3632.
- (40) Casals, E.; Pfaller, T.; Duschl, A.; Oostingh, G. J.; Puentes, V. *Small* **2011**, *Accepted*.
- (41) Salk, D.; Van Wezel, A.; Salk, J. *The Lancet* **1984**, *324*, 1317-1321.
- (42) Sabin, A. B. *J Infect Dis* **1985**, *151*, 420-36.
- (43) Bachmann, M. F.; Rohrer, U. H.; Kundig, T. M.; Burki, K.; Hengartner, H.; Zinkernagel, R. M. *Science* **1993**, *262*, 1448-1451.
- (44) Bachmann, M. F.; Zinkernagel, R. M. *Immunology Today* **1996**, *17*, 553-558.
- (45) Feldmann, M.; Basten, A. *J. Exp. Med.* **1971**, *134*, 103-119.
- (46) Jegerlehner, A.; Storni, T.; Lipowsky, G.; Schmid, M.; Pumpens, P.; Bachmann, M. *European Journal of Immunology* **2002**, *32*, 3305-3314.
- (47) Noad, R.; Roy, P. *Trends in Microbiology* **2003**, *11*, 438-444.
- (48) Johnson, J. E.; Chiu, W. *Current Opinion in Structural Biology* **2000**, *10*, 229-235.
- (49) Newman, M. S.; Colbern, G. T.; Working, P. K.; Engbers, C.; Amantea, M. A. *Cancer Chemotherapy and Pharmacology* **1999**, *43*, 1-7.
- (50) Chen, C.; Daniel, M. C.; Quinkert, Z. T.; De, M.; Stein, B.; Bowman, V. D.; Chipman, P. R.; Rotello, V. M.; Kao, C. C.; Dragnea, B. *Nano Lett.* **2006**, *6*, 611-615.
- (51) Pale-Grosdemange, C.; Simon, E. S.; Prime, K. L.; Whitesides, G. M. *J. Am. Chem. Soc.* **1991**, *113*, 12-20.
- (52) Olmedo, I.; Araya, E.; Sanz, F.; Medina, E.; Arbiol, J.; Toledo, P.; x; lvarez-Lueje, A.; Giralt, E.; Kogan, M. J. *Bioconjugate Chem.* **2008**, *19*, 1154-1163.
- (53) Walczyk, D.; Bombelli, F. B.; Monopoli, M. P.; Lynch, I.; Dawson, K. A. *Journal of the American Chemical Society*, *132*, 5761-5768.
- (54) Bachmann, M. F.; Zinkernagel, R. M.; Oxenius, A. *J Immunol* **1998**, *161*, 5791-5794.
- (55) Janes, K. A.; Calvo, P.; Alonso, M. J. *Advanced Drug Delivery Reviews* **2001**, *47*, 83-97.
- (56) Chavany, C.; Saison-Behmoaras, T.; Doan, T. L.; Puisieux, F.; Couvreur, P.; Hélène, C. *Pharmaceutical Research* **1994**, *11*, 1370-1378.